



Neuroradiology/Head and Neck Imaging Review Article

# Current Management and Image Review of Skull Base Chordoma: What the Radiologist Needs to Know

Erik Soule<sup>1</sup>, Saif Baig<sup>2</sup>, Peter Fiester<sup>1</sup>, Adam Holtzman<sup>3</sup>, Michael Rutenberg<sup>3</sup>, Daryoush Tavanaiepour<sup>4</sup>, Dinesh Rao<sup>1</sup>

Departments of <sup>1</sup>Neuroradiology, <sup>2</sup>Radiology, <sup>3</sup>Radiation Oncology and <sup>4</sup>Neurosurgery, University of Florida College of Medicine, Jacksonville, Florida, United States.



**\*Corresponding author:**

Erik Soule,  
Department of Neuroradiology,  
University of Florida College of  
Medicine, Jacksonville, Florida,  
United States.

[erik.soule@jax.ufl.edu](mailto:erik.soule@jax.ufl.edu)

Received : 08 July 2021  
Accepted : 14 August 2021  
Published : 30 August 2021

DOI  
10.25259/JCIS\_139\_2021

**Quick Response Code:**



## ABSTRACT

Chordomas of the skull-base are typically slow-growing, notochord-derived tumors that most commonly originate along the clivus. Skull base chordoma is treated with surgery and radiotherapy. Local recurrence approaches 50% at 10 years. Radiologists play a critical role in diagnosis, treatment planning, and follow-up. Surgeons and radiation oncologists rely on radiologists for pre-operative delineation of tumor and adjacent anatomy, identification of post-treatment changes and disease recurrence, and radiation treatment effects. This review provides an overview of clinical characteristics, surgical anatomy, indications for radiotherapy, identification of treatment complications, and patterns of disease recurrence for radiologists to provide value in the management of these lesions.

**Keywords:** Chordoma, Magnetic resonance imaging, Computed tomography, Skull base surgery, Radiation therapy

## INTRODUCTION

The objective of this article is to present an anatomic overview of skull base structures, invasion patterns of clival chordoma, surgical planning, post-operative anatomic changes, recognizing recurrent disease, and post-radiation treatment effects, and identifying clinically relevant details for radiologists.

Chordomas are rare, typically indolent tumors arising from embryonic remnants of the primitive notochord.<sup>[1,2]</sup> They can originate along the skull-base, spine or sacral portions of the axial skeleton.<sup>[1]</sup> In a study of 262 patients, chordoma was found to occur most often in the sacrum (50%) followed by sphenoid-occipital (35%) and spinal (15%) locations.<sup>[1,3]</sup>

The incidence of chordoma is 0.08–0.5/100,000 people/year, with skull base location accounting for one case/two million people/year.<sup>[3,4]</sup> Consisting of <0.2% of intracranial neoplasms, skull base chordomas have a higher incidence in younger patients ranging from 20 to 50 years of age and carry a predilection for the female sex.<sup>[5,6]</sup>

Skull base chordomas tend to originate in the sphenoid-occipital synchondrosis of the clivus, which includes the upper or basisphenoid clivus, caudal margin or baso-occipital clivus, or at the petrous apex.<sup>[1]</sup> Less commonly, intradural areas, sella turcica, sphenoid sinus, nasopharynx, maxilla, and paranasal sinuses are sites of origin.<sup>[1]</sup> While conventional histopathologies are

This is an open-access article distributed under the terms of the Creative Commons Attribution-Non Commercial-Share Alike 4.0 License, which allows others to remix, tweak, and build upon the work non-commercially, as long as the author is credited and the new creations are licensed under the identical terms.

©2021 Published by Scientific Scholar on behalf of Journal of Clinical Imaging Science

rarely metastatic, these tumors can spread by local invasion into the skull base, intradural space, and eventually compress the brainstem.<sup>[1]</sup>

As most chordomas have a low frequency of regional or distant metastasis, the prognosis is driven by local recurrence (LR) which approaches 50% at 10 years, often related to the difficulty in achieving gross tumor resection secondary and the ability to deliver dose escalated radiotherapy.<sup>[1,2]</sup>

## CLINICAL PRESENTATION

Due to the slow growth of skull base chordomas, patients often present insidiously. Presenting symptoms will depend on location and extension patterns from the clivus and associated compression of adjacent neurologic and vascular structures.<sup>[1,2]</sup> The most common early complaints are diplopia and occipital or retro-orbital headache. Cranial nerve (CN) II and CN III palsy may also occur and are associated with tumors involving the upper clivus. CN VI induced diplopia may occur with tumors of the mid-clivus and CN IX, X, and XII palsies with tumors for the lower clivus.<sup>[4,7-10]</sup> Brainstem compression may manifest with myelopathic or upper motor neuron signs and symptoms and is accompanied by high morbidity and mortality. Headache is often attributed to trigeminal nerve compression, dural invasion, and increased intracranial pressure.<sup>[2]</sup>

## HISTOPATHOLOGY

There are four histological subtypes of chordoma [Table 1]: Conventional, chondroid, dedifferentiated, and poorly differentiated; however, tumors will often have overlapping histological features.<sup>[2]</sup> Conventional or typical chordomas are the most common variant and are low grade malignancies characterized by cords of physaliphorous neoplastic cells containing intracytoplasmic mucopolysaccharides.<sup>[11]</sup> Chondroid subtypes are characterized by foci of cartilage formation often being described as “islands,” appearing within tumor as hyperintense foci on T1- and T2-weighted MR sequences.<sup>[11]</sup> They are believed to be a form of low-grade chondrosarcoma, and carry the best prognosis of all subtypes.<sup>[12]</sup>

The dedifferentiated subtype is typically aggressive tumors with biphasic characteristics of classic chordoma histology and high-grade sarcomatous features.<sup>[13]</sup> Dedifferentiated subtypes account for 5% of cases and is most often found in pediatric patients, with a 25.4% survival at 5 years.<sup>[14,15]</sup> The poorly differentiated subtype is a more recently recognized aggressive form also seen primarily in pediatric patients, and has an increased tendency for metastasis and LR early in disease.<sup>[13]</sup> Unlike dedifferentiated subtypes, poorly differentiated chordomas are characterized by loss of SMARCB1-INI1 gene expression.<sup>[13]</sup> At many institutions, induction chemo- and radiation therapy (RT) are the initial modes of treatment.<sup>[13]</sup>

Chondroid and conventional subtypes will typically contain areas of necrosis, varying stages of blood degradation products, dystrophic calcification, mucin collections, and entrapped bone trabeculae producing heterogenous signal on T1-weighted MR sequences.<sup>[11]</sup> A hallmark of these lesions is macroscopic hyperintense T2 lobulations, with random non-radial growth.<sup>[11]</sup> In addition, osseous invasion is frequently present within the skull base.<sup>[11]</sup>

## IMAGING CHARACTERISTICS

Based on the relative strengths of computed tomography (CT) and magnetic resonance imaging (MRI), both modalities are required for accurate characterization of clival chordomas and their relationship to adjacent anatomy. MRI is the best modality for radiologic evaluation of intracranial chordomas.<sup>[1,2]</sup> MRI generates intrinsic soft-tissue contrast resulting in excellent characterization of subtle morphologic tumor characteristics, tumor extension, and anatomic involvement. In comparison, CT is limited in resolving soft-tissue structures of the posterior fossa due to beam-hardening artifact.<sup>[1]</sup> MRI is also the modality of choice for identifying intradural extension, an important factor in surgical planning.<sup>[1,11]</sup> T2-weighted sequences are superior in differentiating adjacent neural structures from abutting tumor.<sup>[2]</sup>

Due to the high fluid content of vacuolated components, classic and chondroid skull base chordomas demonstrate hyperintense signal on T2-weighted sequences along with heterogenous hypotense foci associated with mucus, hemorrhage or calcification [Figure 1].<sup>[16]</sup> Lobule formation is a hallmark of chondroid chordoma and is best appreciated on T2-weighted sequences.<sup>[2,11]</sup> These lesions classically demonstrate intermediate to low signal intensity on T1-weighted sequences with small hyperintense foci representing mucus or hemorrhage.<sup>[2]</sup> It is important to note that T2-weighted sequences are more specific, as T1-sequences may show a large variation in signal between cases.<sup>[11]</sup>

Classic and chondroid chordomas will display a honeycomb pattern of enhancement with lines of non-enhancement



**Figure 1:** Contrast-enhanced sagittal T1 (a) and axial T2 (b) MRI exams of a 56-year-old male with a lower clival skull base chordoma (white arrows) with brainstem compression (white stars).

**Table 1:** Imaging and histopathologic characteristics of various chordoma subtypes.

Chordoma subtype	Histology	Image features	Grade
Classic	Cords of physaliphorous neoplastic cells containing intracytoplasmic mucopolysaccharides	Honeycombed enhancement with lines of non-enhancement on contrast-enhanced T1-weighted sequences	Low
Chondroid	Foci of cartilage formation	Similar to classic chordoma. Hyperintense foci on T1 and T2- weighted MR sequences	Low
Dedifferentiated	Biphasic classic chordoma and high-grade spindle-cell or osteosarcoma	T1-isointense to muscle. Hyperintense on T2- weighted sequences.	High, mainly post-RT patients
Poorly differentiated	Sheets of epithelioid cells with eosinophilic cytoplasm	Mainly T2-weighted hypointense signal	High, mainly pediatric and adolescent patients

on contrast-enhanced T1-weighted sequences [Figure 2]. Tumor resolution further improves with the addition of fat suppression.<sup>[16]</sup> Contrast-enhanced sequences should be utilized to characterize tumor extension and differentiation from normal tissue. Hemorrhage or calcification can be confirmed with gradient echo or susceptibility-weighted sequences. Necrosis or cartilage may appear as low intensity septations on T1-weighted sequences.<sup>[16]</sup> Cartilaginous septations will enhance with administration of gadolinium, and necrosis will appear hyperintense on T2.

In contrast, poorly differentiated chordoma demonstrates mainly T2-weighted hypointense signal; however, there is a paucity of literature to establish consistent imaging characteristics [Figure 3].<sup>[14]</sup> The dedifferentiated subtype of chordoma may demonstrate hypointense signal on T2-weighted sequences.<sup>[16]</sup>

Ecchordosis physaliphora can have similar imaging and pathological characteristics to classic chordoma. The distinguishing characteristic between chordoma is the presence of infiltrative growth at the margins in chordoma.<sup>[17]</sup>

Osseous invasion is another hallmark of skull base chordomas. CT is superior to MRI in evaluating bony destruction and osseous invasion, and should be utilized to delineate the extent of bony involvement. This is particularly important in inferior clival chordomas, where tumor may involve the occipital condyles and upper cervical spine.<sup>[11]</sup>

Chordoma metastases occur in 6–30% of chordomas and demonstrate imaging characteristics similar to the primary tumor.<sup>[16]</sup> Metastases may occur in skin, bone, lungs, and liver; however, impact of metastatic disease on prognosis is unclear.<sup>[16]</sup>

## ANATOMIC REVIEW

An understanding of clival anatomy is critical determining local invasion and resectability. Knowledge of proximal structures such as the optic nerves and brainstem is important for radiotherapy planning.

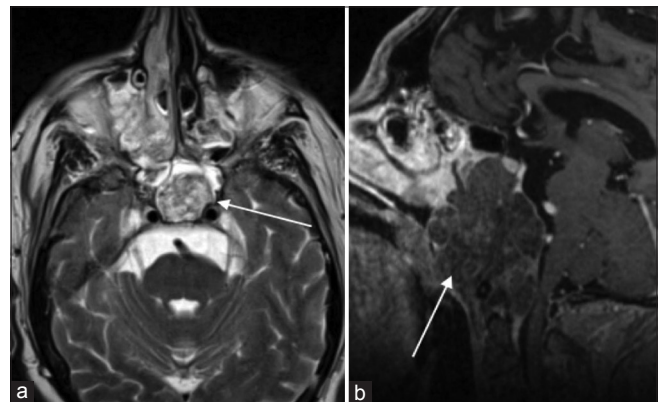


**Figure 2:** Contrast-enhanced axial T2 (a) and sagittal T1 (b) MRI in a 50-year-old male demonstrating a classic chordoma (white arrows) arising from the clivus. Note the honeycomb hyperintense signal on T2-weighted images. The tumor is predominately hypointense on T1-weighted images with a peripheral septal pattern of enhancement.

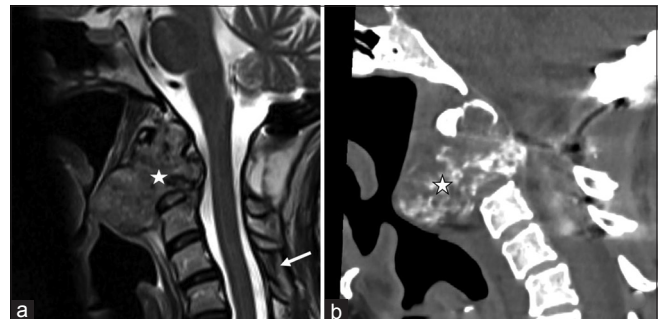


**Figure 3:** Sagittal T2 (a) and sagittal unenhanced CT (b) demonstrating a poorly differentiated chordoma (white star) arising from the C2 vertebral body in a 40-year-old female. Note the hypointense matrix on the sagittal T2 image. The patient had undergone posterior decompression and craniocervical fusion before referral for proton therapy (white arrow). Note the irregular arc and ring pattern of calcification on CT (white star with black border).

While there are various methods in anatomic classification, the Sekhar and Janecka approaches, which divides the



clivus into thirds are the most commonly used for surgical planning.<sup>[18]</sup> The upper clivus is formed from the sphenoid bone. Also called the “sellar” clivus, the upper clivus is made up of the dorsum sella and posterior clinoids, down to the floor of the sella [Figure 4].

The winged sphenoid bone forms the center of the skull base and contains the sella turcica superiorly and upper clivus posteriorly.<sup>[19]</sup> The lateral and medial pterygoid muscles project downward from the sphenoid body on either side. The sella turcica, which houses the pituitary gland, is bounded by the tuberculum sella anteriorly and dorsum sella posteriorly. The paired posterior clinoid processes project from the dorsum sella superolaterally. The medial aspects of the cavernous sinuses form the lateral walls of the sella, containing the paired petrous carotid arteries.<sup>[19]</sup> Dorello’s canal forms the transition boundary between the upper and mid-clivus.

The middle clivus extends from the floor of the sella to the choana. It is bounded by the paraclival internal carotid arteries, the foramen lacerum, and the petroclival fissure [Figure 5]. The mid-clivus forms the anterior border of the prepontine cistern, which contains the basilar trunk, anterior inferior cerebellar artery, abducens nerve (CNIII), and ventral pons.<sup>[19]</sup> Due to the ease of surgical access to the middle clivus, tumors of this region are the easiest to resect with the best probability of achieving gross total resection (GTR).<sup>[20]</sup>

Also known as “nasopharyngeal” clivus, the inferior clivus is part of the occipital bone. It extends from the foramen lacerum to foramen magnum, covering the premedullary cistern and its associated CNs and vasculature anterior to the brainstem. The inferior clivus is attached to the pharyngobasilar fascia, longus capitis and rectus capitis muscles, and surrounded by the jugular foramen, occipital condyles, atlanto-occipital joint, anterior C1 ring, and tectorial membrane.<sup>[19]</sup> Due to proximity to the brainstem and associated neurovasculature, tumors of the inferior clivus, as well as craniocervical junction tumors, have the lowest GTR rates and correspondingly high recurrence.

### EVOLUTION OF SURGICAL APPROACH

Before the advent of highly accurate targeted radiation techniques, surgical and radiation treatments for skull base chordomas could at best provide palliation. Complete tumor resection was rarely possible with surgery alone and radiation treatments could not target specific tissue without considerable radiation-induced injury to adjacent structures.

Surgical procedures for skull base tumors date back to the early 1900s. In 1919, Daland *et al.*<sup>[21]</sup> performed the first documented resection of a spheno-occipital chordoma, which extended from the right ear into the neck, and

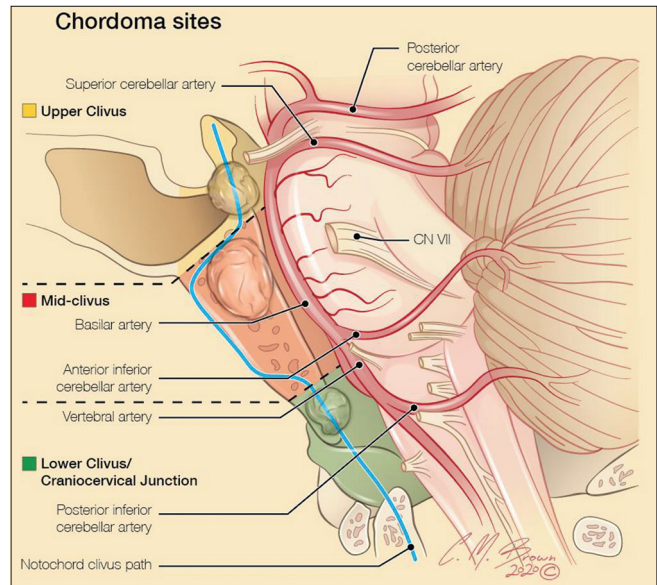


**Figure 4:** Sagittal illustration demonstrating the three divisions of the clivus. The upper clivus extends from the superior aspect of the sella turcica to Dorello’s canal. The mid clivus extends from the inferior border of the sphenoidal sella to the level of the choana. The lower clivus is also known as the “nasopharyngeal clivus” and extends to the craniocervical junction, containing osseous and ligamentous structures.

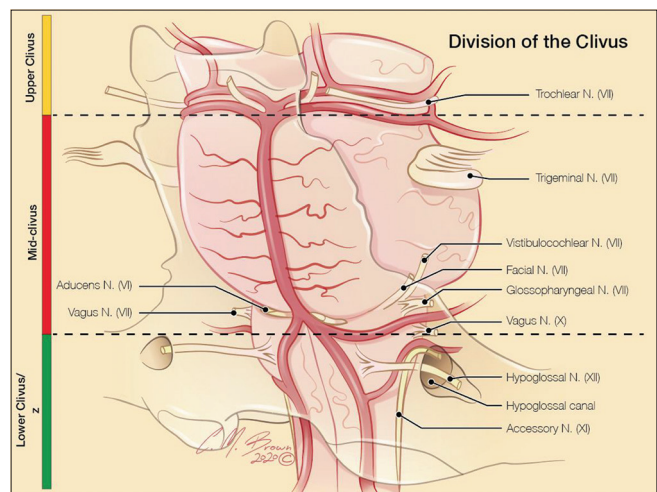


**Figure 5:** Oblique coronal illustration with the surgical divisions of the clivus in silhouette and its anatomic position relative to the brainstem, posterior circulation arterial vasculature and Cranial nerves.

recurred despite radiation treatment.<sup>[21]</sup> In 1918, the first craniotomy was performed for a clival chordoma, followed by the first suboccipital craniotomy and decompression in 1923.<sup>[21]</sup> The first cerebellar craniotomy, transfrontal craniotomy, transsphenoidal resections, and transcervical transclival approach were performed in 1941, 1953, and 1966, respectively.<sup>[22]</sup> These early surgical techniques achieved poor

GTR of tumors; however, the advent of advanced imaging and modern radiotherapy reduced LR rates in skull base chordomas.<sup>[22,23]</sup>

Modern surgical techniques make use of endoscopic endonasal approaches (EEA) techniques for the majority of tumors. However, minimally invasive open techniques may be utilized and are often combined with EEA as staged procedures when performing midline and lateral skull base surgery. The improved anatomic access of modern techniques has allowed for a more complete resection of tumor volume, resulting in improved overall survival (OS) and reduced the rate of LR.<sup>[24]</sup>

## MODERN SURGICAL APPROACHES

Clival chordomas are typically extradural midline tumors that grow dorsally or dorsolaterally.<sup>[25]</sup> Patients with these tumors often present when they are large and extend into multiple compartments requiring the use of multiple approaches when attempting complete resection.<sup>[25]</sup>

Surgical approaches are classified as anterior midline or lateral approaches.<sup>[2,7]</sup> Anterior midline approaches include the extended subfrontal, transmaxillary, transmandibular, EEA, and transcervical approaches. Whereas lateral approaches include frontotemporal orbitozygomatic, anterior transpetrosal, preauricular infratemporal, combined supra- and infratentorial transtemporal, and extreme lateral transcondylar.

In general, extradural surgical techniques are utilized to preserve dural integrity in the absence of tumor involvement. The dura acts as an important barrier to tumor extension. Surgical approaches requiring violation of the dura can seed the surgical tract resulting in recurrent disease. Thus, surgical approaches which require violation of the dura should only be utilized when pre-existing intradural involvement is present.<sup>[7]</sup>

Anterior midline approaches are primarily used for central extradural parts of tumors.<sup>[7]</sup> Lateral skull base approaches are best suited for tumors that extend into the parasellar region, petrous temporal bone, occipital condyle, cavernous sinus, or for tumors that involve the cavernous ICA, vertebrobasilar arteries, or brainstem.<sup>[7]</sup> Due to the predominantly midline location of skull base chordomas, anterior midline surgical approaches are primarily employed and subsequently supplemented with lateral approaches depending on anatomic extension.<sup>[25]</sup>

The development of EEA has changed anatomic designations and routes of open or transcranial surgery.<sup>[26]</sup> EEA allows for access to the central skull base, while reducing the need for craniotomy and brain retraction.<sup>[7,25]</sup> Surgical decision making is largely guided by location and extent of tumor and

its proximity to important anatomic structures. For example, if clival chordomas are localized to the clivus with minimal lateral extension, EEA is sufficient to achieve complete resection. In the presence of significant lateral involvement, lateral transcranial approaches may be required.

LR is related to tumor location and the degree of local invasion into adjacent structures. Having an understanding of anterior, lateral and endoscopic approaches and the resulting anatomic changes secondary to these procedures will reveal patterns of residual tumor after surgery and recurrence. Skull base chordomas will recur from residual tumor or microscopic remnants along the surgical tract or in locations distal to or inaccessible via the chosen approach [Figure 6].

## FOLLOW-UP IMAGING

Identifying residual tumor and distinguishing it from post-treatment changes is important on post-operative imaging. The location and quantification of residual tumor volume have prognostic effects on disease recurrence, and must be identified before RT. In cases where apparent GTR has been achieved, follow-up imaging of primary resection sites after treatment should occur every 6 months for 4–5 years with MRI. Thereafter, every year for 15 years, if patients are disease-free according to the chordoma global consensus group.<sup>[27]</sup>

MRI is the modality of choice for post-treatment follow-up and detection of residual or recurrent disease.<sup>[1]</sup> T2-weighted sequences are useful in detecting remaining or recurrent tumor, especially after the resolution of post-surgical inflammation. Contrast-enhanced sequences allow for improved differentiation of normal post-operative changes and recurrent tumor [Figure 7].<sup>[1]</sup> Consistent imaging protocols during follow-up are also helpful in evaluating for tumor across time.

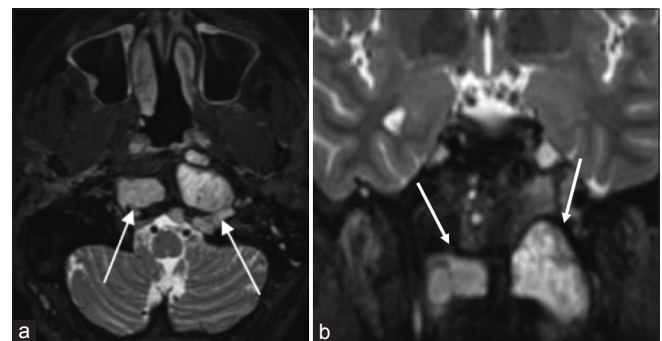


**Figure 6:** Axial STIR (a) and coronal T2 fat saturated (b) images demonstrating residual chordoma (white arrows) in a 36 year old male who had undergone endoscopic endonasal approaches (EEA). The residual tumor was too lateral and inferior to resect during the EEA and was subsequently treated with proton radiation therapy.

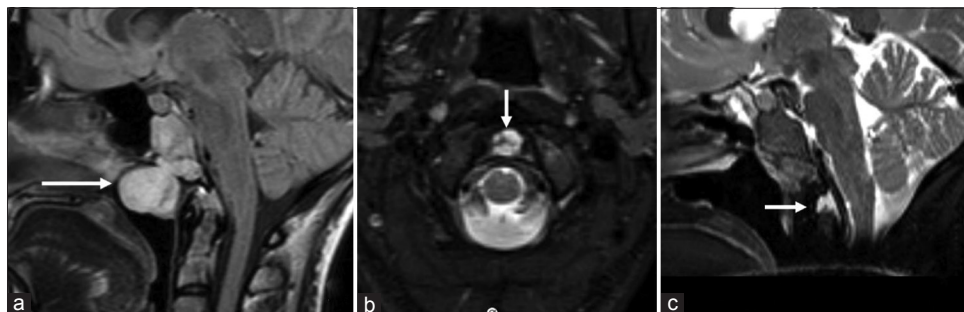


**Figure 7:** Sagittal fluid attenuated inversion recovery (a) MRI demonstrating a chordoma arising from the inferior aspect of the clivus in a 40-year-old female. Note that there is a large nasopharyngeal component (white arrow). Both the clival and nasopharyngeal components of tumor were resected through endoscopic endonasal approaches (EEA). Axial (b) and sagittal (c) STIR MRI demonstrates residual tumor (white arrows) interposed between the basion and odontoid, which was present on preoperative MRI, but not described. Residual chordoma was resected through repeat EEA.

Detection of residual chordoma may be difficult on early post-operative scans due to the presence of blood, surgical packing material, and inflammation.<sup>[28]</sup> This can be especially difficult in T2-hyperintense tumors where inflammation, bony structures and CSF can obscure residual tumor volume [Figure 8].<sup>[28]</sup>

Dynamic contrast-enhanced MR perfusion has also demonstrated utility in monitoring for chordoma growth and response to RT.<sup>[29]</sup>

## RT

Maximal safe resection, ideally with GTR of tumor is the mainstay of treatment. The degree of tumor resection is important in achieving local control (LC), maximizing cause-specific survival, and optimizing the target geometry for safe delivery of adjuvant radiotherapy.<sup>[27]</sup> For those who undergo debulking tumor mass procedures or subtotal resection, tumor decompression is important when critical anatomy such as the CNs, brainstem, and blood vessels is involved. Decompression enhances the effectiveness of RT by allowing for safe dose-escalation to the tumor while sparing adjacent sensitive, non-targeted normal neural tissue.<sup>[30]</sup>

Multimodal therapy with adjuvant RT has been shown to achieve superior LC and OS.<sup>[31]</sup> This benefit is seen even in those with macroscopic GTR. In a retrospective study of 36 cervical chordoma patients conducted by Carpentier *et al.*, LR occurred in 100% of cases at 3 years with surgery alone.<sup>[31]</sup> However, when post-surgical RT was administered even in the setting of GTR, recurrence occurred in 30% of patients at 5 years.<sup>[31]</sup>

The advent of modern RT techniques such as intensity modulated RT, stereotactic radiosurgery (SRS), and proton therapy (PT) has allowed for dose intensification and improved OS, LC, and has decreased radiation toxicity. Modern RT techniques offer superior dose distribution and

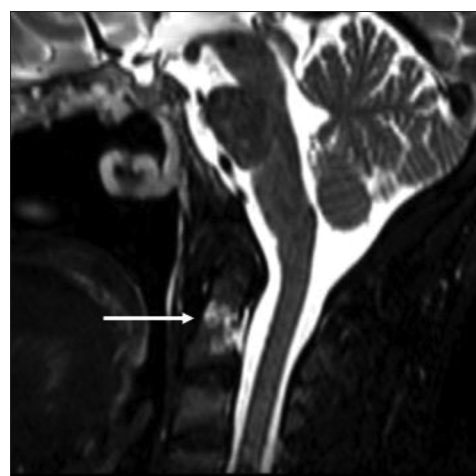


**Figure 8:** A 40-year-old woman with primary chordoma arising from the inferior aspect of the clivus. Sagittal STIR image obtained on surveillance scan 6 months after completion of proton radiation therapy (RT) demonstrating new hyperintense foci (white arrow) within the odontoid process. This was presumed to be tumor and retreated with proton RT.

radiation sparing of adjacent anatomy. In cases where post-RT recurrence manifests, salvage therapy provides little survival benefit.<sup>[30]</sup> In fact, recent NCDB analysis has shown that both dose-escalation and the use of PT improves survival for chordoma and chondrosarcomas.<sup>[32]</sup>

## RT DOSING

Due to the relative radioresistance of chordomas, doses in the range of 70 Gy or more are utilized.<sup>[30]</sup> A retrospective study conducted by Rich *et al.* demonstrated low to moderate-dose RT, i.e. doses <60 Gy, lead to 5-year LC rates of only 28%.<sup>[33]</sup> However, administering optimal doses may be difficult due to adjacent critical neural structures such as the brainstem, optic organs at risk, and upper spinal cord.<sup>[2]</sup> Thus, debulking tumor in areas such as the brainstem, optic pathways, and



spinal cord is the most important factor in achieving LC and OS.<sup>[34]</sup> A space of 1–2 mm between residual disease and adjacent critical structures will typically allow for adequate target coverage with minimal iatrogenic damage.<sup>[30]</sup>

## RT PLANNING

Radiation oncologists rely on various volumetric measurements when contouring tumor and outlining treatment fields [Figure 9].<sup>[35]</sup> Gross tumor volumes (GTV) represent residual tumor on pre-RT treatment imaging. The clinical tumor volume (CTV) represents GTV and surrounding margins encompassing probable microscopic disease. CTV dimensions are formulated on a combination of clinical judgment, histopathology, tumor aggression, pattern of spread, and location of adjacent lymph nodes.<sup>[35]</sup> Final planning target volume (PTV) represents the full contour where RT will be administered. PTV takes systemic and random uncertainties into account, such as potential organ motion, and changes in positioning between co-registered imaging modalities.<sup>[35]</sup> Radiation oncologists rely on radiologists to most accurately define GTV and its relation to adjacent anatomy to improve contour accuracy, particularly in cases where surgery has altered the appearance of native anatomy.

## PRE-TREATMENT IMAGING

Target volumes are contoured exclusively on thin-slice CT scans (1 mm thickness) with and without IV-contrast.<sup>[30]</sup> CT simulation scans provide electron density distributions required for modeling RT planning.<sup>[35]</sup> If soft-tissue resolution is required when contouring, T1 and T2-weighted MR 1 mm thickness slices are co-registered with simulation CTs.<sup>[30]</sup> MR sequences typically include contrast enhanced T1 with fat suppression, fluid attenuated inversion recovery, and conventional T2-sequences.<sup>[30]</sup>

## PT

Improvements in photon-based therapies have allowed for dose intensification and improvements in LC and OS in skull-base chordoma patients. PT is able to deliver conformational RT doses (60 Gy or above) to tumor volumes due to steep dose drop-off outside the border of the targeted area, improving OS and LC over modern photon-based techniques.<sup>[30]</sup> In a systematic review conducted by Amichetti *et al.*, average 5 year LC and OS was 69.2% and 79.8% with PT, compared with 36% and 53.5% with conventional RT, 50% and 82% with SRS, and 56% and 75% with gamma-knife radiosurgery.<sup>[36]</sup> A recent retrospective study by Palm *et al.* demonstrated a 5 year OS of 100% with high dose PT compared to 34% with conventional RT.<sup>[32]</sup> Dose conformality and RT delivery characteristics allow for relatively safe treatment of tumors abutting the optic nerves and optic chiasm using PT.<sup>[30]</sup>

## RADIATION COMPLICATIONS

Radiation complications occur with increasing probability when normal tissues are exposed to doses of radiation. They can occur either as a threshold limits with a specific organ tolerance or a linear no threshold model also known as deterministic or stochastic effects. Treatment effects predominately occur within the treatment field and correspond to dose distribution. Follow-up imaging search patterns should take into account the mapping of initial RT fields. In the context of skull-base tumors, important dose limiting normal tissues include brain, brainstem, upper cervical spine, optic nerves and chiasm, eyes, cochlea, temporal-mandibular joint, CNs III-XII, salivary, and lacrimal glands.<sup>[37]</sup> Severity of clinical symptoms of radiation effects serve as the basis for toxicity grading, and include temporal hair loss, headache of various degrees, visual degradation, loss of appetite, fatigue, nausea, vomiting, and sinusitis and is often scored per the CTCAE or RTOG guidelines.<sup>[38]</sup>

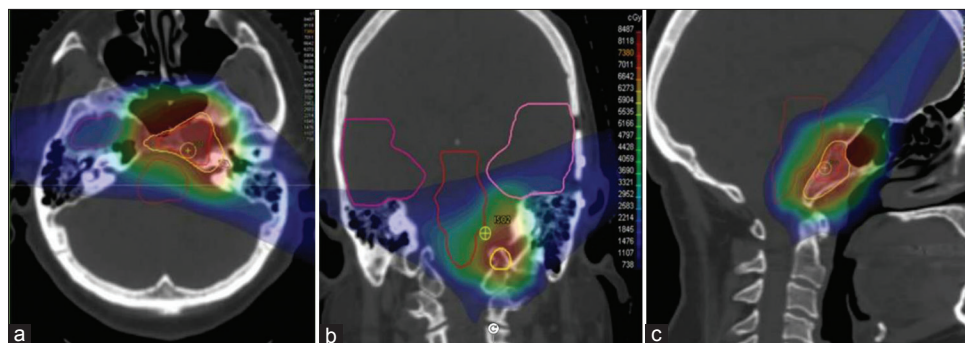


**Figure 9:** Planning scan with isodose dose distribution and the Gross Tumor Volume (GTV, red shading) and Clinical Target Volume (yellow shading) expansion in a patient with skull base chondrosarcoma. Normal organs depicted are the cochlea, brainstem and temporal lobes (outlines). The plan prescription dose is 73.8 at 1.8 GyRBE with a 3 mm isotropic expansion for Planning Target Volume and a reduction to GTV after 50.4 GyRBE.

While low rates of acute toxicity have been reported with radiation, late toxicity is well documented and occurs in the range of 8–17% of cases. Although PT is used for mitigating normal tissue exposure, late effects such as cerebral necrosis, visual deficits, pituitary insufficiency, and hearing loss may occur due to tumor overlap, placing these structures in the PTV.<sup>[39]</sup> The role of surgery to optimize target geometry for safe dose escalation with adjuvant radiotherapy is therefore critical.

Radiation-related late treatment effects involving brain, brainstem, and upper cervical spinal cord can result in severe morbidity or even death.<sup>[37,39]</sup> Brainstem and cerebral necrosis have been shown to occur at a mean interval of 17 months, with majority of these patients experiencing symptoms within 3 years [Figure 10].<sup>[40,41]</sup> Clinical symptoms have been documented to occur as long as 7 years after irradiation.<sup>[42]</sup>

Most cases of cerebral necrosis involve the temporal lobe (TL), and have an 8% and 13% probability of occurring at 2 and 5 years post-treatment, respectively. Most patients with cerebral necrosis will exhibit symptoms related to white matter changes, such as slowed psychomotor reaction time and decreased motor speed.<sup>[39]</sup> A subset of patients may develop TL epilepsy secondary to parenchymal scarring, manifesting on a continuum of severity ranging from transient seizures to status epilepticus. Imaging findings range from white matter changes to areas of parenchymal necrosis on MRI.<sup>[42]</sup> Depending on the grade of TL injury, MRI examination may demonstrate increased T2W signal in the anterior TL, with posterior or medial extension [Figure 11].<sup>[42]</sup> In Grade IV TL injury, diffuse coalescence of white and grey matter may be seen, associated with T2 hyperintense signal, loss of cerebral architecture and cortical atrophy.<sup>[42]</sup> MR findings correlate superiorly with clinical presentation in comparison to CT findings.<sup>[43]</sup> Patients with seizures may be managed with medical therapy; however, surgical resection of injured tissue may be required in refractory cases.<sup>[42]</sup> Cerebral necrosis is typically managed with steroids, pentoxifylline, and Vitamin E.<sup>[44]</sup>

Cervical myelopathy may occur in a minority of post-proton RT cervical chordoma patients at a mean follow-up period of 46.5 months.<sup>[45]</sup> CN palsies may also occur with probability increasing with radiation dose.<sup>[36]</sup>

In retrospective study conducted by Kim *et al.* including 274 chordoma patients given RT with a median dose of 62.1 Gy, the incidence of optic neuropathy was 4.4%.<sup>[45]</sup> Visual deficits presented as early as 10 months and as late as 34 months post-treatment [Figure 12].<sup>[46]</sup>

In a study evaluating 33 patients receiving iatrogenic RT to the cochlea or auditory nerves, more than two-thirds of the patients experienced rapid, severe hearing loss 2–5 years post-treatment when the dose exceeded 62.5 Gy.<sup>[47]</sup> Hearing

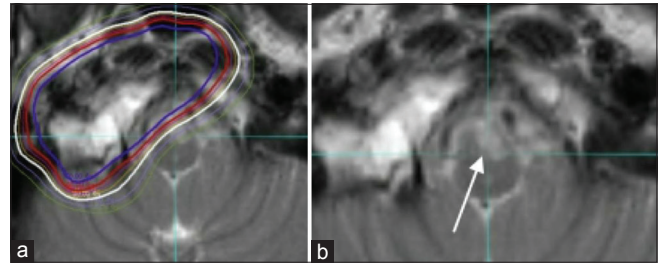


**Figure 10:** Axial T2 images from radiation therapy planning (a) and 20 month follow-up (b) scans on a patient with a right petroclival residual chordoma demonstrating hyperintense T2 signal (white arrow) within the left ventral medulla interpreted as brainstem necrosis.

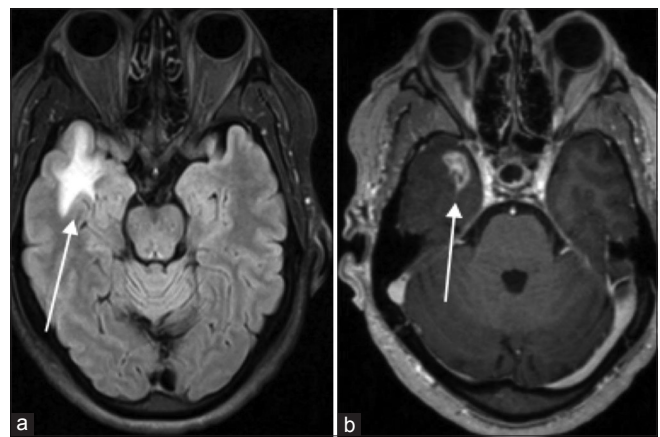


**Figure 11:** Axial fluid attenuated inversion recovery (a) and contrast-enhanced T1 SPGR (b) MRI in 55-year-old male with chordoma status post endoscopic resection and residual tumor treated with proton radiation therapy (RT); temporal lobe necrosis (white arrows) 2 years after completion of RT.

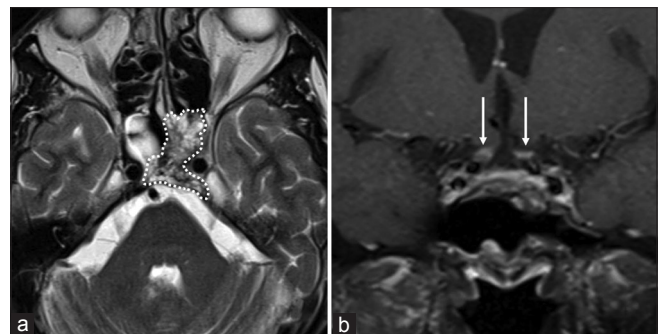


**Figure 12:** Axial (a) T2 MR image of a 63-year-old female with residual tumor (white outline) in the left cavernous sinus and dorsum sellae after endoscopic endonasal approaches. The patient underwent proton radiation therapy (RT) for the residual tumor. Coronal (b) T1 fat saturated MR image demonstrating enhancement of the bilateral optic nerves (white arrows) 2 years after completion of RT. The patient had complained of visual changes and eventually completes vision loss.



loss is typically ipsilateral, especially if RT involves the petroclival synchondrosis.

In midline upper clival tumors, pituitary insufficiency such as LH, prolactin, TSH, and/or ACTH deficiency may result from radiation-induced pituitary injury. Slater *et al.* reported that 50% of patients receiving doses of 67.6 Gy showed complications between 14 and 45 months, with some cases presenting up to 8–10 years later.<sup>[37,48]</sup>

## SECONDARY BRAIN TUMORS

Advances in surgical techniques and adjuvant chemoradiation have provided major survival benefit for cancer patients. RT produced ionizing radiation is carcinogenic and has been shown to increase the risk of secondary neoplasms in long-term cancer survivors.<sup>[49]</sup> Radiation induced neoplasms are uncommon late iatrogenic effects typically attributed to childhood cancer treatment, and carry an incidence of <1% in adults.<sup>[50]</sup>

Radiation-induced meningiomas (RIM), radiation-induced sarcoma (RIS), and radiation-induced gliomas are the most common secondary brain tumors.<sup>[51]</sup> RIMs are more aggressive than spontaneous meningiomas and have a median latency period of 18.8 years with high dose RT (>30 Gy).<sup>[52,53]</sup> Imaging findings on MR and CT examinations are similar to those seen with spontaneous meningiomas.<sup>[53]</sup> RIS typically arise from irradiated bone, dura, and leptomeninges.<sup>[54,55]</sup> These tumors carry a poor prognosis and have a median latency period of 10.8 years with high dose RT.<sup>[54]</sup> Radiation-induced gliomas are a rare complication of cranial irradiation with an incidence of 0.5–2.7% up to 15 years post-treatment, with mean latency period of 9 years.

## CONCLUSION

Conventional clival chordomas are slow-growing malignant tumors that are locally aggressive with 10-year local progression approaching 50%. The best treatment outcomes include maximal safe resection, followed by dose-escalated RT. A combination of CT and MR information is utilized to characterize tumor extension into the skull base and its relationship to surrounding neuroanatomy. Skull base tumor resection is most commonly accomplished with a combination of anterior, endoscopic, and lateral approaches. Radiation treatment planning requires accurate assessment of residual disease volumes and quantitative distance of residual tumor from critical anatomy such as the brainstem, CNs, and cervical spine. The neuroradiologist has a central role in identifying initial/residual disease, disease recurrence, and treatment complications. Recognizing imaging findings of treatment complications such as brainstem/TL necrosis, optic/cranial neuropathies, and cervical myelopathy are essential.

## Declaration of patient consent

Patient's consent not required as patients identity is not disclosed or compromised.

## Financial support and sponsorship

Nil.

## Conflicts of interest

There are no conflicts of interest.

## REFERENCES

1. Erdem E, Angtuaco EC, van Hemert R, Park JS, Al-Mefty O. Comprehensive review of intracranial chordoma. *Radiographics* 2003;23:995-1009.
2. Koutourousiou M, Snyderman CH, Fernandez-Miranda J, Gardner PA. Skull base chordomas. *Otolaryngol Clin North Am* 2011;44:1155-71.
3. McMaster ML, Goldstein AM, Bromley CM, Ishibe N, Parry DM. Chordoma: Incidence and survival patterns in the United States, 1973-1995. *Cancer Causes Control* 2001;12:1-11.
4. Crockard HA, Steel T, Plowman N, Singh A, Crossman J, Revesz T, *et al.* A multidisciplinary team approach to skull base chordomas. *J Neurosurg* 2001;95:175-83.
5. Huvos AG. *Bone Tumors: Diagnosis, Treatment and Prognosis*. 2<sup>nd</sup> ed. United States: WB Saunders; 1987. Available from: [http://www.inis.iaea.org/search/search.aspx?orig\\_q=rn:18094791](http://www.inis.iaea.org/search/search.aspx?orig_q=rn:18094791). [Last accessed on 2021 Mar 23].
6. Higinbotham, NL, Phillips, RF, Farr, HW, Hutsu, HO. Chordoma. Thirty-five-year study at memorial hospital. *Cancer* 1967;20:1841-50.
7. Sen C, Triana AI, Berglind N, Godbold J, Shrivastava RK. Clival chordomas: Clinical management, results, and complications in 71 patients. *J Neurosurg* 2010;113:1059-71.
8. Gay E, Sekhar LN, Rubinstein E, Wright DC, Sen C, Janecka IP, *et al.* Chordomas and chondrosarcomas of the cranial base: Results and follow-up of 60 patients. *Neurosurgery* 1995;36:887-7.
9. Colli B, Al-Mefty O. Chordomas of the craniocervical junction: Follow-up review and prognostic factors. *J Neurosurg* 2001;95:933-43.
10. Stippler M, Gardner PA, Snyderman CH, Carrau RL, Prevedello DM, Kassam AB. Endoscopic endonasal approach for clival chordomas. *Neurosurgery* 2009;64:268-8.
11. Pamir MN, Özduman K. Analysis of radiological features relative to histopathology in 42 skull-base chordomas and chondrosarcomas. *Eur J Radiol* 2006;58:461-70.
12. Brooks JJ, LiVolsi VA, Trojanowski JQ. Does chondroid chordoma exist? *Acta Neuropathol* 1987;72:229-35.
13. Shih AR, Cote GM, Chebib I, Choy E, DeLaney T, Deshpande V, *et al.* Clinicopathologic characteristics of poorly differentiated chordoma. *Mod Pathol* 2018;31:1237-45.
14. Beccaria K, Tauziède-Espariat A, Monnier F, Adle-Biassette H, Masliah-Planchon J, Pierron G, *et al.* Pediatric chordomas: Results of a multicentric study of 40 children and proposal for a

- histopathological prognostic grading system and new therapeutic strategies. *J Neuropathol Exp Neurol* 2018;77:207-15.
15. Hoch BL, Nielsen GP, Liebsch NJ, Rosenberg AE. Base of skull chordomas in children and adolescents: A clinicopathologic study of 73 cases. *Am J Surg Pathol* 2006;30:811-8.
  16. Santegoeds RG, Temel Y, Beckervordersandforth JC, van Overbeeke JJ, Hoerberigs CM. State-of-the-art imaging in human chordoma of the skull base. *Curr Radiol Rep* 2018;6:16.
  17. Mehnert F, Beschorner R, Küker W, Hahn U, Nägele T. Retroclival echordosis physaliphora: MR imaging and review of the literature. *AJNR Am J Neuroradiol* 2004;25:1851-5.
  18. Sekhar LN, Jannetta PJ, Burkhart LE, Janosky JE. Meningiomas involving the clivus: A six-year experience with 41 patients. *Neurosurgery* 1990;27:764-81; discussion 781.
  19. Patel CR, Fernandez-Miranda JC, Wang WH, Wang EW. Skull base anatomy. *Otolaryngol Clin North Am* 2016;49:9-20.
  20. Zoli M, Milanese L, Bonfatti R, Faustini-Fustini M, Marucci G, Tallini G, *et al.* Clival chordomas: Considerations after 16 years of endoscopic endonasal surgery. *J Neurosurg* 2017;128:329-38.
  21. Daland EM: Chordoma. *Boston Med Surg J* 180:571-6, 1919.
  22. Zoltan L, Fenyés I. Stereotactic diagnosis and radioactive treatment in a case of sphenoparietal chordoma. *J Neurosurg* 1960;17:888-900.
  23. Mazzoni A, Krengli M. Historical development of the treatment of skull base tumours. *Rep Pract Oncol Radiother* 2016;21:319-24.
  24. Tamaki N, Nagashima T, Ehara K, Motooka Y, Barua KK. Surgical approaches and strategies for skull base chordomas. *Neurosurg Focus* 2001;10:E9.
  25. Carrabba G, Dehdashti AR, Gentili F. Surgery for clival lesions: Open resection versus the expanded endoscopic endonasal approach. *Neurosurg Focus* 2008;25:E7.
  26. Fernandez-Miranda JC, Gardner PA, Snyderman CH, Devaney KO, Mendenhall WM, Suárez C, *et al.* Clival chordomas: A pathological, surgical, and radiotherapeutic review. *Head Neck* 2014;36:892-906.
  27. Stacchiotti S, Gronchi A, Fossati P, Akiyama T, Alapetite C, Baumann M, *et al.* Best practices for the management of local-regional recurrent chordoma: A position paper by the chordoma global consensus group. *Ann Oncol* 2017;28:1230-42.
  28. Guler E, Ozgen B, Mut M, Soylemezoglu F, Oguz KK. The added value of diffusion magnetic resonance imaging in the diagnosis and posttreatment evaluation of skull base chordomas. *J Neurol Surg B Skull Base* 2017;78:256-65.
  29. Santos P, Peck KK, Arevalo-Perez J, Karimi S, Lis E, Yamada Y, *et al.* T1-weighted dynamic contrast-enhanced MR perfusion imaging characterizes tumor response to radiation therapy in chordoma. *AJNR Am J Neuroradiol* 2017;38:2210-6.
  30. Mercado CE, Holtzman AL, Rotondo R, Rutenberg MS, Mendenhall WM. Proton therapy for skull base tumors: A review of clinical outcomes for chordomas and chondrosarcomas. *Head Neck* 2019;41:536-51.
  31. Carpentier A, Polivka M, Blanquet A, Lot G, George B. Suboccipital and cervical chordomas: The value of aggressive treatment at first presentation of the disease. *J Neurosurg* 2002;97:1070-7.
  32. Rich TA, Schiller A, Suit HD, Mankin HJ. Clinical and pathologic review of 48 cases of chordoma. *Cancer* 1985;56:182-7.
  33. Fung V, Calugaru V, Bolle S, Mammari H, Alapetite C, Maingon P, *et al.* Proton beam therapy for skull base chordomas in 106 patients: A dose adaptive radiation protocol. *Radiother Oncol* 2018;128:198-202.
  34. Terezakis SA, Heron DE, Lavigne RF, Diehn M, Loo BW. What the diagnostic radiologist needs to know about radiation oncology. *Radiology* 2011;261:30-44.
  35. Amichetti M, Cianchetti M, Amelio D, Enrici RM, Minniti G. Proton therapy in chordoma of the base of the skull: A systematic review. *Neurosurg Rev* 2009;32:403-16.
  36. Palm RF, Oliver DE, Yang GQ, Abuodeh Y, Naghavi AO, Johnstone PA. The role of dose escalation and proton therapy in perioperative or definitive treatment of chondrosarcoma and chordoma: An analysis of the national cancer data base. *Cancer* 2019;125:642-51.
  37. Munzenrider JE, Liebsch NJ. Proton therapy for tumors of the skull base. *Strahlenther Onkol* 1999;175:57-63.
  38. Alahmari M, Temel Y. Skull base chordoma treated with proton therapy: A systematic review. *Surg Neurol Int* 2019;10:96-2019.
  39. Sze G, Uichanco LS 3<sup>rd</sup>, Brant-Zawadzki MN, Davis RL, Gutin PH, Wilson CB, *et al.* Chordomas: MR imaging. *Radiology* 1988;166:187-91.
  40. Holtzman AL, Rotondo RL, Rutenberg MS, Indelicato DJ, Mercado CE, Rao D, *et al.* Proton therapy for skull-base chondrosarcoma, a single-institution outcomes study. *J Neurooncol* 2019;142:557-63.
  41. Hug EB, Loredano LN, Slater JD, DeVries A, Grove RI, Schaefer RA, *et al.* Proton radiation therapy for chordomas and chondrosarcomas of the skull base. *J Neurosurg* 1999;91:432-9.
  42. Debus J, Hug EB, Liebsch NJ, O'Farrell D, Finkelstein D, Efid J, *et al.* Brainstem tolerance to conformal radiotherapy of skull base tumors. *Int J Radiat Oncol Biol Phys* 1997;39:967-75.
  43. Santoni R, Liebsch N, Finkelstein DM, Hug E, Hanssens P, Goitein M, *et al.* Temporal lobe (TL) damage following surgery and high-dose photon and proton irradiation in 96 patients affected by chordomas and chondrosarcomas of the base of the skull. *Int J Radiat Oncol Biol Phys* 1998;41:59-68.
  44. Constine LS, Kanski A, Ekholm S, McDonald S, Rubin P. Adverse effects of brain irradiation correlated with MR and CT imaging. *Int J Radiat Oncol Biol Phys* 1988;15:319-30.
  45. Kim JK, Leeman JE, Riaz N, McBride S, Tsai CJ, Lee NY. Proton therapy for head and neck cancer. *Curr Treat Options Oncol* 2018;19:28.
  46. Habrand JL, Austin-Seymour M, Birnbaum S, Wray S, Carroll R, Munzenrider J, *et al.* Neurovisual outcome following proton radiation therapy. *Int J Radiat Oncol Biol Phys* 1989;16:1601-6.
  47. Schoenthaler R, Fullerton BC, Maas AV, Collier JM, Liebsch NJ, Hug EB, *et al.* Relationship between dose to auditory pathways and audiological outcomes in skull-base tumor patients receiving high-dose proton-photon radiotherapy. *Int J Radiat Oncol Biol Phys* 1996;36:291.
  48. Slater JD, Austin-Seymour M, Munzenrider J, Birnbaum S, Carroll R, Klibanski A, *et al.* Endocrine function following high dose proton therapy for tumors of the upper clivus. *Int J Radiat Oncol Biol Phys* 1988;15:607-11.
  49. Tubiana M. Can we reduce the incidence of second primary malignancies occurring after radiotherapy? A critical review. *Radiother Oncol* 2009;91:4-15.

50. Galloway TJ, Indelicato DJ, Amdur RJ, Morris CG, Swanson EL, Marcus RB. Analysis of dose at the site of second tumor formation after radiotherapy to the central nervous system. *Int J Radiat Oncol Biol Phys* 2012;82:90-4.
51. Ron E, Modan B, Boice JD, Alfandary E, Stovall M, Chetrit A, *et al.* Tumors of the brain and nervous system after radiotherapy in childhood. *N Engl J Med* 1988;319:1033-9.
52. Yamanaka R, Hayano A, Kanayama T. Radiation-induced gliomas: A comprehensive review and meta-analysis. *Neurosurg Rev* 2018;41:719-31.
53. Umansky F, Shoshan Y, Rosenthal G, Fraifeld S, Spektor S. Radiation-induced meningioma. *Neurosurg Focus* 2008;24:E7.
54. Yamanaka R, Hayano A, Kanayama T. Radiation-induced meningiomas: An exhaustive review of the literature. *World Neurosurg* 2017;97:635-44.e8.
55. O'Regan K, Hall M, Jagannathan J, Giardino A, Kelly PJ, Butrynski J, *et al.* Imaging of radiation-associated sarcoma. *AJR Am J Roentgenol* 2011;197:W30-6.

**How to cite this article:** Soule E, Baig S, Fiester P, Holtzman A, Rutenberg M, Tavaniaepour D, *et al.* Current management and image review of skull base chordoma: What the radiologist needs to know. *J Clin Imaging Sci* 2021;11:46.